Desalination and Water Treatment
www.deswater.com
doi: 10.1080/19443994.2015.1093550

57 (2016) 18939–18955
August

Taylor & Francis
Taylor & Francis Group

Removal of pyridine from dilute aqueous streams using hollow fiber supported liquid membranes

A.G. Yewale, N.D. Patil, A.W. Patwardhan*

Department of Chemical Engineering, Institute of Chemical Technology, Matunga, Mumbai 400019, India, emails: ayewale07@gmail.com (A.G. Yewale), ndp.chem@gmail.com (N.D. Patil), Tel. +91 22 33612018; Fax: +91 22 33611020; email: aw.patwardhan@ictmumbai.edu.in (A.W. Patwardhan)

Received 12 February 2015; Accepted 5 September 2015

ABSTRACT

The removal of pyridine from aqueous phase using hollow fiber supported liquid membranes has been investigated. Effect of several parameters such as feed concentration, extractant concentration, type of extractants, etc. has been studied. Organic solvents such as, 2-nonyl phenol (2-NP), 4-nonyl phenol (4-NP), stearic acid (SA), and di-(2-ethylhexyl) phosphoric acid (D2EHPA) were used as extractants. It was observed that the initial flux of pyridine increased with an increase in extractant concentration. The investigations showed that phenolic-based extractants (4-NP or 2-NP) were better for pyridine removal as compared to other extractants. The equilibrium experiments have been carried out by varying stirring speed and time in order to find the reaction kinetics and equilibrium time. Mass transfer-based model was used to explain the removal of pyridine for three different modules. Scale-up experiment shows nearly similar flux values of pyridine at both the scales. The model results were found to be in good agreement with the experimental observations. The results have been explained on the basis of steric effects, acidity of the extractant molecules along with the overall mass transfer resistance for the transport of pyridine.

Keywords: Pyridine; Supported liquid membranes; Flux; Separation; Mass transfer; Model

1. Introduction

Pyridine is a basic heterocyclic organic compound mainly used as precursor to agrochemicals and pharmaceuticals. It is also an important solvent used in the manufacture of different pharmaceutical compounds, vitamins, pesticides, paints, dyes, rubber products, adhesives, etc. Pyridine is usually present in effluents from rubber, plastics, petrochemicals, pharmaceuticals, and agrochemicals industries. The pyridine concentration in the industrial effluents can be as high as 500 mg/dm^3 (0.006 kmol/m^3) [1]. Beyond 0.82 mg/dm^3 unpleasant pyridine odor can be easily detected [2]. Removal of pyridine from effluent aqueous streams is important from environmental point of view. Pyridine is very bioactive and highly soluble in water [3]. It has poor biodegradability in water; thus it increases the toxicity of water. Pyridine exposure causes several chronic effects on liver, kidney, and reproductive functions [4–6]. Many of the pyridine compounds are considered hazardous and remain in environment for long duration. Therefore, it is essential to remove pyridine from aqueous stream with a suitable and efficient technique.

*Corresponding author.

1944-3994/1944-3986 © 2015 Balaban Desalination Publications. All rights reserved.

Separation of pyridine has been studied by a number of researchers using conventional techniques such as, adsorption [6–8], liquid–liquid extraction [9], chemical oxidation, and biodegradation [10,11]. Each of these techniques has some limitations. For example, liquid–liquid extraction requires large quantities of solvent; chemical oxidation produced toxic products, while adsorption and biodegradation methods cannot be used for high concentration of pyridine [12]. Pyridine and water form azeotrope at 366.6 K with a molar composition of 0.245 kmol/m^3 of pyridine [13]. Distillation is an inefficient technique for pyridine removal from water due to high energy consumption and limitations of azeotrope.

Joyce et al. [14] studied the separation of pyridine from water solution using silicalite-filled silicone composite membrane. Drioli et al. [13] studied the recovery of pyridine from aqueous solution by pervaporation technique. These studies showed that the flux of pyridine increases with an increase in feed concentration. Singha et al. [15] employed filled styrene butadiene rubber membrane for the removal of pyridine from water. They observed that, the increase in filler loading results in increase in the pyridine selectivity. Based on these studies it can be concluded that the pyridine flux and selectivity for membrane separation processes are the functions of several parameters such as feed concentration, filler concentrations, nature of membrane material, etc.

Kujawski et al. [16] employed several ion exchange membranes, containing carboxylic, and sulfonic functional groups for the dehydration of aqueous pyridine solution. They found that, the transport mode and selectivity are dependent on ion exchange group and the ionic form of membranes. Lee and Oh [17] carried out a series of experiments for separating water from aqueous pyridine solution.

Several studies have been carried out for the removal of pyridine and its derivatives using commercially available adsorbents. Adsorbents such as granular activated carbon (GAC) [18], zeolites [19], sepiolite [20], and activated carbon from coconut shells and fibers [21,22] were found useful for pyridine removal from effluent. Lataye et al. [7] examined the adsorption of pyridine from synthetic aqueous solutions by rice husk ash (RHA) and commercial grade GAC. They found that, the adsorption of pyridine was higher for GAC compared to RHA. The studies on adsorption of pyridine including kinetics, equilibrium, and thermodynamics aspects have been reported.

Extraction mechanism of pyridine and its substituted form like cynopyridine (CP) using phenol as extractant has been discussed [23,24]. The pyridine nitrogen is mainly responsible for complexation, due to its strong interaction with –OH group of phenol. It was also observed that the nitrogen in nitrile functional group might interact with phenolic proton [25]. Phenolic-based extractants like 4-nonyl phenol (4-NP), 2-nonyl phenol (2-NP), etc. have lower solubility in aqueous phase due to their strong hydrophobic nature. For these reasons phenolic-based extractants have been tested in the present study for the pyridine removal. In addition, acidic extractants like stearic acid (SA) and di-(2-ethylhexyl) phosphoric acid (D2EHPA) have been tried for removal of pyridine from dilute aqueous solutions.

Supported liquid membrane (SLM) is a technique in which organic extractants is immobilized with membrane support. Aqueous stream is fed on one side of the membrane, while on the other side a strip solution is fed. The solute gets extracted from the feed aqueous phase into the organic extractant contained in the membrane and gets stripped from the membrane phase into the strip solution. In recent years, the application of SLM has been increased because of its low solvent inventory, single unit separation, and relatively low energy requirement [26–28]. Adsorption-based separations also require a separate regeneration step, whereas, SLM-based separations combine the extractant and regeneration steps in a single unit.

To the best of our knowledge, no work has been carried out to date on the hollow fiber supported liquid membrane (HFSLM) process for removal of pyridine from aqueous waste streams. The novelty of this work lies in the methodology that has been followed: (i) liquid–liquid extraction experiments are carried out to measure the distribution coefficient of pyridine under various conditions, (ii) development of a mathematical model, and (iii) predictions based on the model for different modules and at two scales.

2. Experimental

2.1. Materials

Pyridine (99.5%), 2-nonyl phenol (2-NP), 4-nonyl phenol (4-NP), di-(2-ethylhexyl) phosphoric acid (D2EHPA), stearic acid (SA), dodecane, kerosene, and HCl were obtained from S.D. Fine Chemical Ltd India. All the chemicals were of AR grade and used without further purification. Deionized water (Millipore) was used to prepare feed solutions throughout the study. Hollow fiber polypropylene (PP) membrane module was procured from Membrana, Charlotte, USA. Three different Liqui-Cel modules, X40 (0.28 m^2 area), and

X50 (0.45 and 3.24 m^2 area) are used in the present work. The specifications of hollow fiber membrane modules are given in Table 1.

2.2. Equilibrium study

Equilibrium experiments of pyridine with various extractants were carried out to find the extraction equilibrium constants (K_{ex}) and distribution coefficients (k). In order to check the effect of diluents on pyridine removal, dodecane and kerosene were used as diluents to dilute organic extractants. Aqueous phases were prepared at various concentration of pyridine in deionized water, in the range 0.005–0.03 kmol/m^3. This range covers the typical pyridine concentrations found in aqueous effluent streams. Organic phases were prepared from the organic extractant such as 2-NP, 4-NP, D2EHPA, and SA and the diluents dodecane or kerosene. Table 2 shows the structure and acidity of different extractants.

Equal volumes (1.5 ml) of aqueous phases containing different pyridine concentrations (0.005–0.03 kmol/m^3) were mixed with the organic phases containing different extractant concentrations (0.01–0.1 M) at 298 K. After shaking the mixture vigorously for 1 h, both the phases were allowed to settle and then separated by centrifugation at 1,000 rpm (100 g). In order to find the kinetics of the reaction, the equilibrium experiments were performed at various stirring speed by withdrawing samples at different intervals of time. The aqueous samples containing pyridine were removed at 200, 500, and 1,000 rpm stirring speed. Absorbance of the samples was measured at wavelength of 256 nm using UV–vis spectrophotometer to determine the pyridine concentration [6]. The concentration data obtained from these experiments have been used for the calculation of K_{ex}.

2.3. Transport of pyridine through HFSLM

Experimental setup consisted of one HFSLM module, two reservoirs and two peristaltic pumps (one each for feed and strip solution) is identical to our previous work [29]. The liquid membrane phase was prepared by pumping organic extractants solution through the lumen side of the module in recirculation mode. For proper impregnation of organic liquid inside membrane pore, the organic liquid was pumped from lumen side (inlet), with the outlet of the lumen side closed. The organic liquid thus permeated from lumen to shell side through the pores of the membrane. After finishing one set of pyridine removal experiments; the loaded organic was removed by washing with kerosene before loading another organic liquid. Once a particular organic phase is loaded onto the membrane, several pyridine removal experiments were carried out. This indicates that the "loaded" membrane is stable.

Aqueous feed and strip phases were prepared using different concentration of pyridine and HCl acid in deionized water, respectively. About 0.1 kmol/m^3 HCl acid solution was used as strip phase for all the experiments. The flow rate of feed/strip phase was controlled using peristaltic pump and experiments were performed at different flow rates. The flow rates studied are 50, 200, 300, and 500 ml/min. During the experimental runs, feed solution was passed through the lumen side, whereas strip solution was passed through the shell side in a countercurrent flow. The exit solutions from the module were recycled back to the respective reservoirs. Approximately 2 ml of sample

Table 1
Specifications of HFSLM modules for removal experiments

Membrane type	Module 1 PP X50 (2.5 × 8)	Module 2 PP X40 (2.5 × 8)	Module 3 PP X50 (4 × 13)
Number of fibers (N)	10,000	10,000	48,000
Fiber internal radius (r_i), μm	120	100	120
Fiber outer radius (r_o), μm	150	150	150
Effective module outer diameter (d_a), cm	4.67	4.67	–
Effective module inner diameter (d_i), cm	2.2	2.2	–
Effective pore size (r_p), μm	0.03	0.03	0.03
Porosity (ε), %	40	25	40
Membrane thickness, μm	30	50	30
Tortuosity (τ)	2.5	2.5	2.5
Effective fiber length (L), cm	15	15	27
Membrane effective surface area (A), m^2	0.45	0.28	3.24

Table 2
Physical properties of organic extractants

Extractant	Structural formula	pK_a	M.W (gm/mol)
4-NP	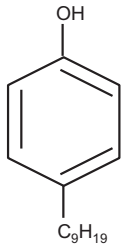	10.28	220.35
2-NP	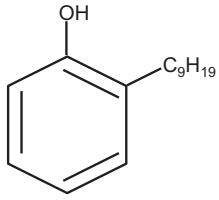	10.28	220.35
SA	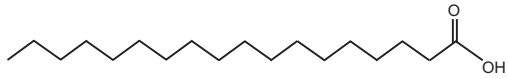	4.75	284.48
D2EHPA	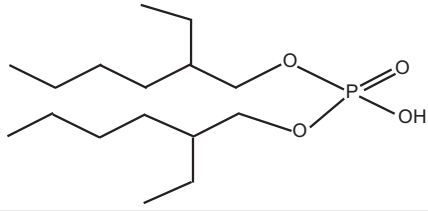	1.47	322.43

was taken from both the feed and the strip phase reservoirs at regular time intervals. The feed phase samples containing pyridine were analyzed using UV-absorbance technique. All the experiments were reproducible in the range of ±5%.

Regarding solvent loss; the solubility of pure nonyl phenol in water is 6 ppm. The solubility of the extractants becomes smaller when organic diluent such as dodecane or kerosene is used. During experimentation, we did not encountered any visual organic layer in any of the feed or strip aqueous phases. Also the experiments were reproducible which corroborates that there is no loss of organic phase.

3. Model equations

A mathematical model developed earlier [30] by considering the mass transfer and the complexation–decomplexation reaction has been extended in the present work to pyridine removal. The details of the model have been given in our earlier work [30]. The overall mass transfer flux (R_T) from feed to strip phase is written in terms of driving force for pyridine transport and the resistances for mass transfer (feed side film resistance and the diffusional resistance through the membrane),

$$R_T = \frac{C_f}{\frac{1}{k_f} + \frac{d_0}{D_m}\left(\frac{1}{k}\right)} = K \,.\, C_f \tag{1}$$

where "K" is defined as the overall mass transfer coefficient for the transport process.

$$\frac{1}{K} = \frac{1}{k_f} + \frac{d_0}{D_m}\left(\frac{1}{k}\right) \tag{2}$$

At the strip side, pyridine reacts instantaneously with HCl to form pyridine hydrochloride. Thus, it can be assumed that the concentration of pyridine at the strip side is zero.

The final form of differential equation for the concentration change with respect to time can be expressed from the material balance of feed phase reservoir,

$$\frac{dC_{f0}}{dt} = \frac{Q_f}{V_f}(C_{fz} - C_{f0}) \tag{3}$$

where C_{fz} is the feed phase (lumen side) module outlet concentration,

$$C_{fz} = C_{f0}\ \exp\left(\frac{-2\varepsilon\,.\,K\,.\,L}{r_{if}u_f}\right) \tag{4}$$

To evaluate K, it is necessary to know the values of "k" and "D_m". These have been estimated as given below.

3.1. Estimation of model parameters (k and D_m)

At the feed-membrane interface pyridine forms a complex with acidic extractant in the organic phase. In general, this reaction can be written as:

$$\mathrm{Py} + \mathrm{nEXT} \rightleftharpoons \mathrm{Py}\cdot\mathrm{nEXT}_{(org)} \tag{5}$$

where Py stands for pyridine and $[\mathrm{Py}\cdot\mathrm{nEXT}]_{(org)}$ is the pyridine-extractant complex.

The extraction equilibrium constant (K_{ex}) is expressed as:

$$K_{ex} = \frac{[\mathrm{Py}\cdot\mathrm{nEXT}]_{org}}{[\mathrm{Py}]_{aq}\cdot[\mathrm{EXT}]^{n}_{free,org}} \tag{6}$$

The reaction equilibrium on the feed-membrane interface is:

$$K_{ex} = \frac{C_{imf}}{C_{if}\cdot[\mathrm{EXT}]^{n}_{free,org}} \tag{7}$$

Mass balance of the extractant (EXT) in the membrane phase may be expressed as:

$$[\mathrm{EXT}]_{initial,org} = [\mathrm{EXT}]_{free,org} + \mathrm{n}[\mathrm{Py}\cdot\mathrm{nEXT}]_{org} \tag{8}$$

Distribution coefficient (k) is calculated from Eq. (6),

$$k = K_{ex}\cdot[\mathrm{EXT}]^{n}_{free,org} = \frac{C_{imf}}{C_{if}} \tag{9}$$

Membrane diffusivity (D_m) signifies diffusion coefficient of the pyridine-complex diffusing through the SLM. In the present work, D_m was estimated by fitting the developed model with the base case of single experiment and the same has been used for making predictions for all other cases [28].

4. Results and discussion

4.1. Equilibrium study

The relationship between distribution coefficient (k) and the equilibrium pyridine concentration in the aqueous phase with 2-NP and 4-NP as extractants are shown in Fig. 1(a) and (b), respectively. It can also be seen from the figures that an increase in the extractant concentration results in an increase in k of pyridine. From Fig. 1(a) and (b) it is evident that the k values of pyridine with phenolic extractants (2-NP or 4-NP) reduce with an increase in the pyridine concentration. At low pyridine concentration, large numbers of extractant molecules are available for complexation with pyridine molecules. As a result, higher k values are observed at low pyridine concentration and vice versa. Comparison of Fig. 1(a) and (b) show that the values of k with 4-NP (1.35–5.91) are higher than those with 2-NP (0.92–3.17).

Values of K_{ex} for pyridine are calculated from the slope of the plot shown in Fig. 1(c) and (d) using Eq. (6). The pyridine-extractant stoichiometry was found to be 1:1. The value of K_{ex} with 4-NP as extractant is higher (60.45 m^3/kmol) compared to 2-NP (47.82 m^3 /kmol). This effect may be attributed to the presence of long alkyl chain at second position in phenolic ring (2-NP). Because of steric hindrance, complex formation with 2-NP becomes difficult as compared to 4-NP. Similarly, the equilibrium experiments were carried out using SA and D2EHPA as extractants. The values of k and K_{ex} obtained from equilibrium study for different organic extractants are given in Table 3. From Table 3 it is found that the k and K_{ex} values are higher for phenolic-based extractants (2-NP or 4-NP) compared to SA and D2EHPA extractants. Plot of K_{ex} vs. pK_a of different organic extractants (Fig. 2) show an interesting relationship. At lower acidity (high pK_a), it shows higher value of

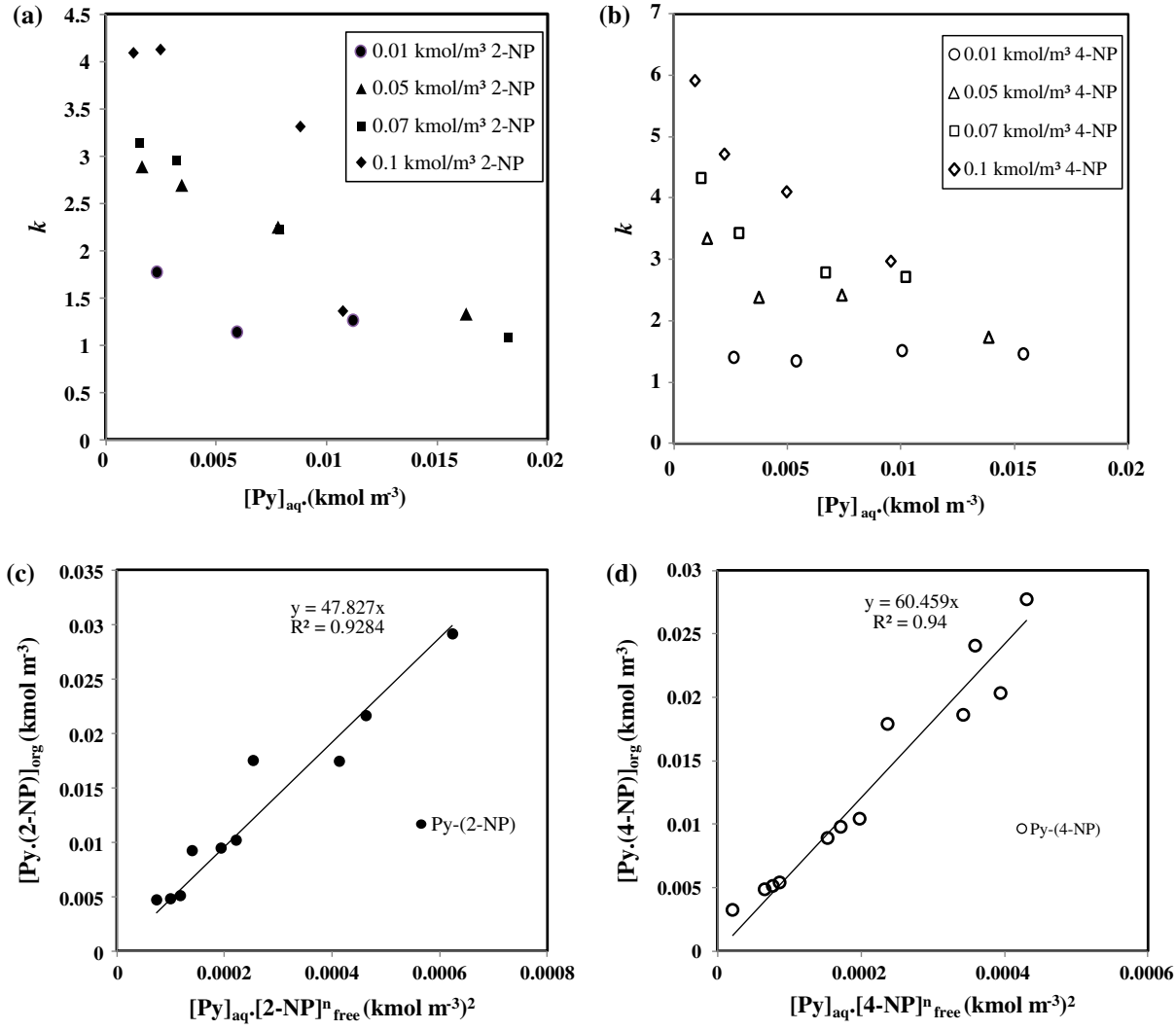

Fig. 1. Distribution coefficient (k) for (a) Py-2-NP system, (b) Py-4-NP system and equilibrium constantstant (K_{ex}) for (c) Py-2-NP system, (d) Py-4-NP system.

Table 3
Equilibrium study of pyridine with different organic extractants

Extractant	Diluent	Distribution coefficient (k)	K_{ex} (m^3/kmol)
D2EHPA	Kerosene	0.25–2.22	9.18
SA	Kerosene	1.6–2.31	28.80
2-NP	Dodecane	1.07–4.12	47.82
2-NP	Kerosene	0.92–3.17	45.65
4-NP	Kerosene	1.35–5.91	60.45

Note: In all the cases the feed phase pyridine concentrations have been varied in the range of 0.005–0.03 kmol/m^3 and pyridine: extractant stoichiometry was found to be 1:1.

K_{ex} and vice versa. The order of acidic strength of organic extractants is D2EHPA > SA > NP (Table 2). Pyridine is a weak Lewis base with one hydrogen bond acceptor in the ring. It favors weak acid-weak base interaction. As a result, 4-NP or 2-NP shows higher K_{ex} value as compared to SA and D2EHPA

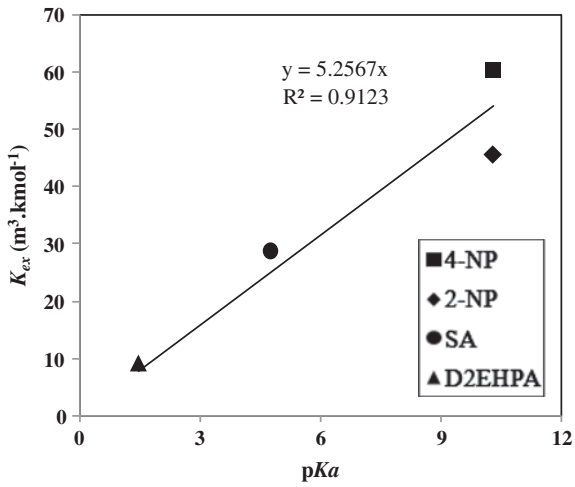

Fig. 2. Effect of pK_a value of different organic extractants on equilibrium constant (K_{ex}).

(Fig. 2). Another reason is that, strongly acidic extractants like D2EHPA [31] and SA [32] exist in a dimerized form in nonpolar diluents such as kerosene, hexane, dodecane, etc. Thus, although D2EHPA and SA have higher acidity, they are not free for complexation with pyridine. The measured values of pH for 0.005 and 0.03 kmol/m^3 pyridine solutions are 7.3 and 8.1, respectively. The dissociation constant of SA and D2EHPA are 0.03380 and 0.000017, respectively. The two extractants can become partially neutralized. In fact the transport of pyridine is through the acid–base complex between pyridine and acidic extractants. However, dimerization of these extractants is likely to be the major reason for the lesser extraction of pyridine using DEHPHA and SA extractants. It can also be seen from Table 3 that the nature of the diluents (dodecane or kerosene) does not significantly affect the values of k and K_{ex}.

The equilibrium experiments were also performed by varying stirring speed and time. This study is performed at 200, 500, and 1,000 rpm stirring speed. The aqueous samples containing pyridine were removed at equal interval of time (10–40 s). This study shows that at higher stirring speed (1,000) the time required to reach 95% of the equilibrium value is less than 10 s. This means that the characteristic time for reaction is about 2–3 s. This means that the rate of complexation reaction is much faster as compared to the mass transfer rate through the pores. It is thus reasonable to assume that the overall process can be modeled based on mass transfer resistances along with very rapid kinetics.

4.2. Model predictions

The experimental data generated with initial concentration of 0.005 kmol/m^3 pyridine in the aqueous phase and 0.01 kmol/m^3 4-NP (diluted in kerosene) as extractant, is selected as base case (Fig. 3(a)). Molecular diffusion coefficient (D) and film mass transfer coefficient (k_f) of pyridine in the aqueous phase are calculated using correlations mentioned by Vernekar et al. [28]. The values of D and k_f are 1.02×10^{-9} m^2/s and 9.80×10^{-6} m/s, respectively. These values have been incorporated in model equations for the calculation of interfacial concentrations. The value of membrane diffusivity (D_m) is fitted in the model so that the predicted values match with the experimental data. The fitted value of membrane diffusivity for the pyridine-4-NP complex through the membrane was found to be 3×10^{-10} m^2/s. This value has been used to predict the concentration data for the validation of remaining set of experimental data. Fig. 3(a) shows the value of diffusivity through the membrane gives excellent match between the model predictions and experimental data.

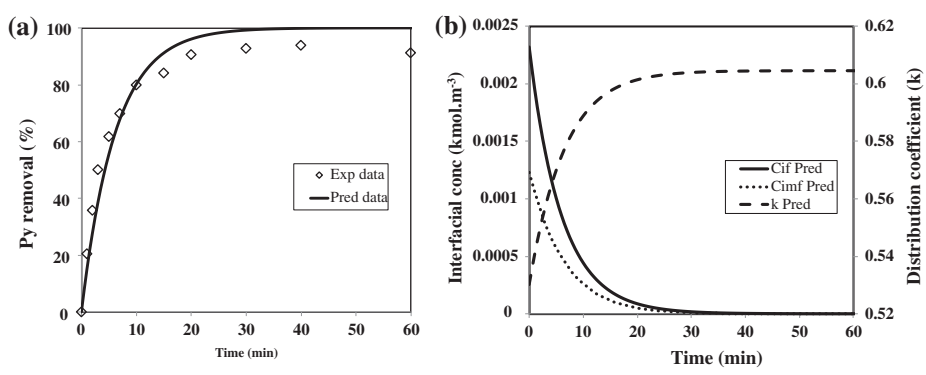

Fig. 3. Pyridine profiles for the base case and model predictions: (a) pyridine removal (%) and (b) pyridine interfacial concentration and distribution coefficient (feed phase: 0.005 kmol/m^3 pyridine solutions (500 ml); organic phase: 0.01 kmol/m^3 4-NP in kerosene; strip phase: 0.1 kmol/m^3 HCl solution (500 ml); feed/strip phase flow rates: 200 ml/min, module 1).

Model predictions enable us to understand the variation of interfacial concentrations and distribution coefficients (k) with time (Fig. 3(b)). Fig. 3(b) shows the relationship between the pyridine concentrations (C_{if}) at the feed-membrane interface and time. It is observed that the values of C_{if} decreases with time. This decrease is due to the depletion of pyridine from the bulk of the feed phase. With time, the reaction equilibrium shifts towards the reduced formation of complex. As a result, the pyridine complexation (C_{imf}) also decreases with time (Fig. 3(b)). As the pyridine concentration drops, the distribution coefficient increases with time. The initial decrease in C_{if} is higher in comparison to decrease in C_{imf}. Therefore, rapid increase in k is observed initially and then it attains a constant value after 20 min.

4.3. Effect of feed phase concentration

The effect of feed phase pyridine concentration on removal of pyridine is studied in the range of 0.005–0.02 kmol/m^3. This study is performed with 4-NP (0.01 kmol/m^3) as extractant diluted in kerosene (Fig. 4(a)). The velocities of solutions through lumen and shell sides of module were kept constant to 0.0074 and 0.0053 m/s, respectively. Fig. 4(a) shows the relationship between extent of pyridine removal and time for 0.01 kmol/m^3 4-NP extractant. It can be seen from the figure that the extent of pyridine removal increases with an increase in time. It is also noticed that the model predictions are in good agreement with the experimental observations. The figure shows that about 40 to 60 min are required for complete removal of pyridine at this range of concentrations. The relationship between overall mass transfer coefficient (K) and time over the used range of pyridine concentrations (0.005–0.02 kmol/m^3) using Eq. (2) is depicted in Fig. 4(b). Eq. (3) shows the correlation between concentration gradient and overall mass transfer coefficient (K). "K" is a combination of (i) feed side mass transfer coefficient (k_f), (ii) membrane diffusivity (D_m) and most importantly, (iii) the distribution coefficient (k). Out of these parameters, k_f and D_m are independent of the concentration of pyridine. The "K" value is

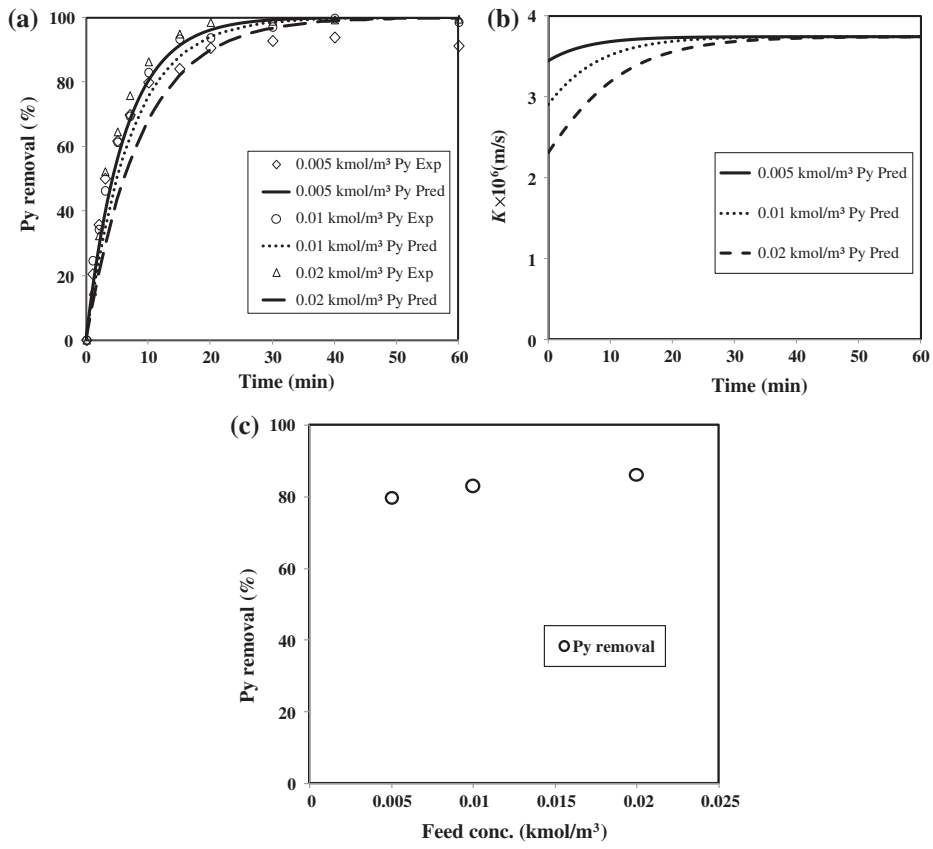

Fig. 4. Effect of feed phase pyridine concentration on (a) pyridine removal (%), (b) Overall mass transfer coefficient (K) and (c) Pyridine removal vs. feed concentration at the end 10 min. (Feed phase, 0.005–0.02 kmol/m^3 pyridine solutions (500 ml); Organic phase, 0.01 kmol/m^3 4-NP in kerosene solution; Strip phase, 0.1 kmol/m^3 HCl solution (500 ml); Feed/Strip phase flow rates, 200 ml/min, Module 1).

strongly affected due to the distribution coefficient (k) of pyridine. As concentration of pyridine in the feed phase becomes close to zero, the distribution coefficient "k" approaches to a very large value. In Eq. (9), the ratio of C_{if}/C_{imf} becomes very large. This is because, at low concentrations of pyridine, the ratio of concentration of the free extractant is very large. As a result of this, the overall mass transfer coefficient "K" increases with a decrease in the concentration of pyridine on the feed side. "K" signifies a combined effect of physical mass transfer "k_f" and the distribution coefficient "k". It can be observed from Fig. 4(b) that, overall mass transfer coefficient (K) is similar in magnitude for the entire range of pyridine concentration after 30–40 min. As a result, similar trends of pyridine removal are observed in Fig. 4(a).

The relationship between extent of pyridine removal vs. feed concentration is shown in Fig. 4(c). The results are plotted at the end of 10 min. Fig. 4(c) shows increase in pyridine removal with an increase in feed concentrations. However, this change is not significantly larger. This could be because of nearly similar values of K over the used concentration range of pyridine.

4.4. Effect of extractant concentration

The plot of extent of pyridine removal vs. time for various extractant concentrations is shown in Fig. 5(a). This study is performed using 0.01–0.1 kmol/m^3 2-NP extractant concentrations. Two different modules (Module 1 and 2) given in Table 1 are used in this study. The results obtained from both these modules show good match between experimental and predicted data. Fig. 5(a) shows that the pyridine removal is more at high extractant concentration. This behavior can be explained on the basis of mass transfer model. The relationship between overall mass transfer coefficient (K) of pyridine and time for 0.01–0.1 kmol/m^3 2-NP concentrations is shown in Fig. 5(b). According to the Eq. (1), the overall mass transfer coefficient (K) is proportional to overall mass transfer flux (R_T), which result into increase in extent of pyridine removal (Eq. (3)). The

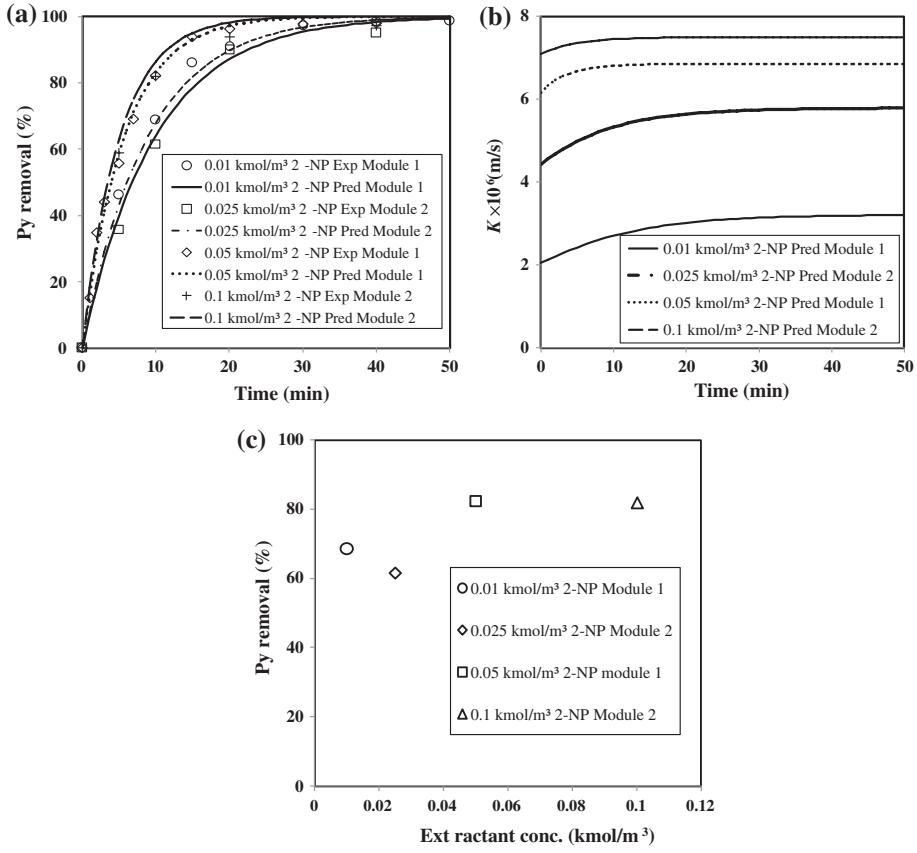

Fig. 5. Effect of extractant concentration on (a) pyridine removal (%), (b) overall mass transfer coefficient (K), and (c) pyridine removal vs. extractant concentration at the end of 10 min (feed phase: 0.02 kmol/m^3 pyridine solutions (500 ml); organic phase: 0.01–0.1 kmol/m^3 2-NP solution; strip phase: 0.1 kmol/m^3 HCl solution (500 ml); feed/strip phase flow rates: 200 ml/min).

value of K at high extractant concentration (0.05–0.1 kmol/m^3) is approximately threefold than at low extractant concentration (0.01 kmol/m^3). Beyond 0.05 M extractant concentration, experimental data shows almost similar trends. This could be because of sufficient moles of extractant molecules were available for complexation with pyridine at high extractant concentration. As a result, the initial flux values observed for 0.02 kmol/m^3 pyridine at 0.01, 0.025, 0.05, and 0.1 kmol/m^3 2-NP are 1.25×10^{-8} (kmol/m^2 s), 3.29×10^{-8} kmol/m^2 s, 6.15×10^{-8} kmol/m^2 s, and 6.10×10^{-8} kmol/m^2 s, respectively. Approximately, 98% of pyridine removal is achieved using 0.05–0.1 kmol/m^3 2-NP at the end of 15 min. It takes longer to achieve 98% of pyridine removal using 0.01–0.025 kmol/m^3 2-NP.

The relationship between extent of pyridine removal and extractant concentration is shown in Fig. 5(c). It can be seen from the figure that the extent of pyridine removal increases with an increase in extractant concentration and it attained maximum value (82%) at 0.05–0.1 kmol/m^3 of 2-NP. The active surface area of membrane (Module 1) is 0.45 m^2 and the thickness of the hollow fiber is 30 μm. The maximum quantity of organic liquid immobilized inside membrane support is about 10–15 ml. Extractant molecules are not immobilized but trapped inside the membrane pore by capillary pressure. The maximum concentration of the organic extractant is 0.1 kmol/m^3 2-NP. Therefore, number of pyridine moles transported per mole of the impregnated organic extractant is 6.6.

4.5. Effect of feed/strip flow rate

The feed and strip flow rates were varied in the range of 50–500 ml/min. The velocity and pressure across lumen and shell sides of the hollow fiber membrane for different flow rates are given in Table 4. It can be seen from Table 4 that the pressure and velocity across module increases with an increase in flow rates. The maximum values of velocity (u_f) and pressure (P_f) across lumen side were found to be 0.0184 m/s and 5,434 N/m^2, respectively, at flow rate of 500 ml/min. Similarly, the maximum value of velocity (u_s) and pressure (P_s) across shell side were found to be 0.0133 m/s and 1,963 N/m^2, respectively, at flow rate of 500 ml/min. The pressure developed due this range of flow rates (50–500 ml/min) is significantly smaller than the breakthrough pressure (9,000 N/m^2) of organic liquid across the hollow fiber membrane pores. The flow rate beyond 700 ml/min across lumen side can be transferred out the membrane fluid. Henceforth the operating flow rate was selected in a such way that, which will corresponds to the pressure below its transmembrane pressure limit.

The relationship between extent of pyridine removal and time for various feed/strip flow rate is shown in Fig. 6(a). It can be seen from Fig. 6(a) that the extent of pyridine removal increases with an increase in flow rate. The extent of pyridine removal for 50-ml/min flow rate is lower compared to 200–500 ml/min. This behavior can be explained using model predictions from Eq. (2). The plot between overall mass transfer coefficient (K) and time for various flow rates is depicted in Fig. 6(b). It can be seen from the plot that the overall mass transfer coefficient (K) increases with an increase in flow rate. The flow rate below 200 ml/min shows lower K values, which leads to reduce the extent of pyridine removal. Beyond 200 ml/min no significant change in K values observed (Fig. 6(b)). Therefore, all the experiments in the present study are carried out with optimized flow rate of 200 ml/min.

The effect of velocity on mass transfer coefficient (K) and extent of pyridine removal is shown in Fig. 6(c). The concentration of pyridine was kept constant at 0.005 M during this study. It can be seen from the figure that the K value increases with an increase in velocity, which leads to increase in extent of pyridine removal. The maximum value of pyridine removal (80–90%) was observed at the velocity ranging from 0.0074 to 0.0184 m/s.

4.6. Effect of hollow fiber module parameters

The effect of porosity (ε), fiber length (L), and membrane thickness (d_0) on extent of pyridine

Table 4
Lumen/shell side velocity and pressure calculated for different flow rates

	Feed/lumen side		Strip/shell side	
Flow rate (ml/min)	Velocity (u_f) (m/s)	Pressure (P_f) (N/m^2)	Velocity (u_s) (m/s)	Pressure (P_s) (N/m^2)
50	0.0019	579	0.0014	196
200	0.0074	1,976	0.0053	741
300	0.0110	3,211	0.0080	1,178
500	0.0184	5,434	0.0133	1,963

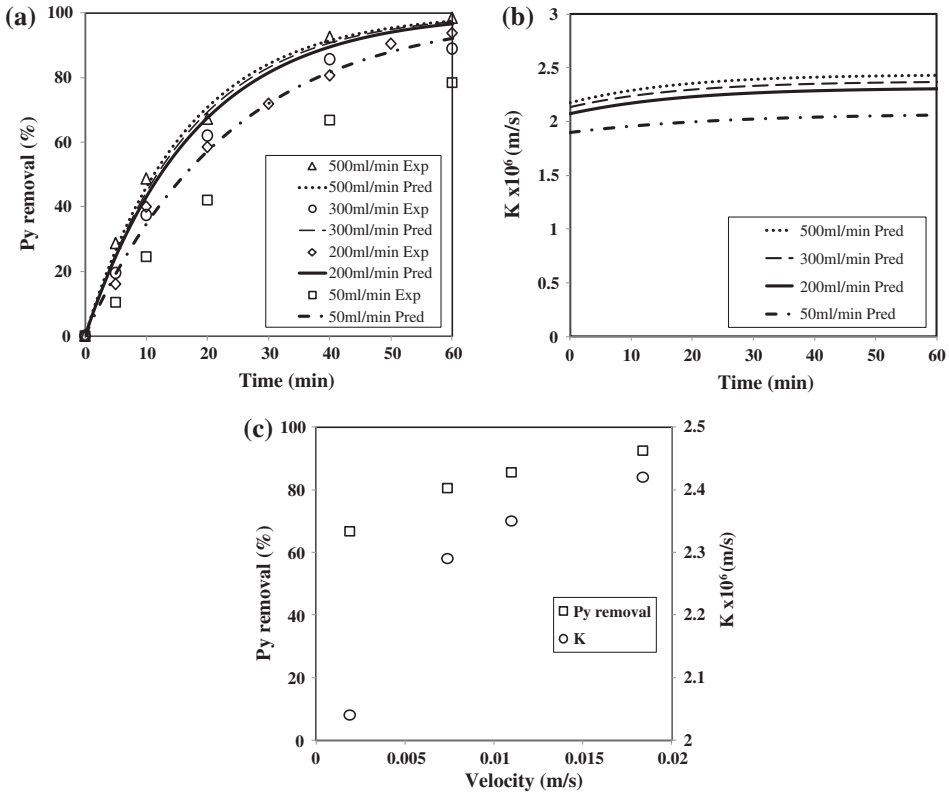

Fig. 6. Effect of flow rate on (a) pyridine removal (%), (b) overall mass transfer coefficient (*K*), and (c) effect of velocity at the end of 40 min (feed phase: 0.005 kmol/m^3 pyridine solution (500 ml); organic phase: 0.01 kmol/m^3 SA solution; strip phase: 0.1 kmol/m^3 HCl solution (500 ml); feed/strip phase flow rates: 50–500 ml/min, module 2).

removal is shown in Table 5. This study is carried out using 0.01 kmol/m^3 pyridine and 0.01 kmol/m^3 SA concentrations. It can be seen from Table 5 that the extent of pyridine removal increases with an increase in porosity and fiber length. This behavior can be understood from the model predictions using Eq. (3). Eq. (3) shows the correlation between concentration gradient and module parameters. With increase in porosity and fiber length, the membrane effective area increases. This results in higher mass transfer rate. As a result, the extent of pyridine removal is higher at high values of porosity and fiber length. The porosity and fiber length does not significantly affect the overall mass transfer coefficient (*K*). It is also observed from Table 5 that the extent of pyridine removal decreases with an increase in membrane thickness. Membrane thickness plays an important role in mass transfer operations. With increase in membrane thickness, the mass transfer resistance across the membrane phase increases, which lead to decrease in mass transfer coefficient (Eq. (2)). As a result, the extent of pyridine removal is high at lower value of membrane thickness (Table 5).

4.7. Comparison of different organic extractants

The effect of different extractants on the removal of pyridine is studied using organic solvents 2-NP, 4-NP, SA, and D2EHPA. This study is performed with 0.005 kmol/m^3 pyridine at constant extractant concentration (0.01 kmol/m^3). The stoichiometry ratio of pyridine with different organic extractants was found to be 1:1. With 0.1 M HCl solution in the strip side, it is possible to enrich the pyridine by a factor of 5–10 times the feed value. The relationship between extent of pyridine removal and time for different organic extractants is depicted in Fig. 7(a). It can be seen from the figure that the extent of pyridine removal is higher for 4-NP and 2-NP extractants compared to D2EHPA and SA extractants. Equilibrium studies (Table 3) and pK_a plot (Fig. 2) can be used to understand the interaction behavior of pyridine with different organic extractants. The distribution coefficients of pyridine with 4-NP and 2-NP extractants are higher than those obtained with D2EHPA and SA extractants. This suggests that the interaction of 4-NP and 2-NP solvents with pyridine is much better than D2EHPA and SA.

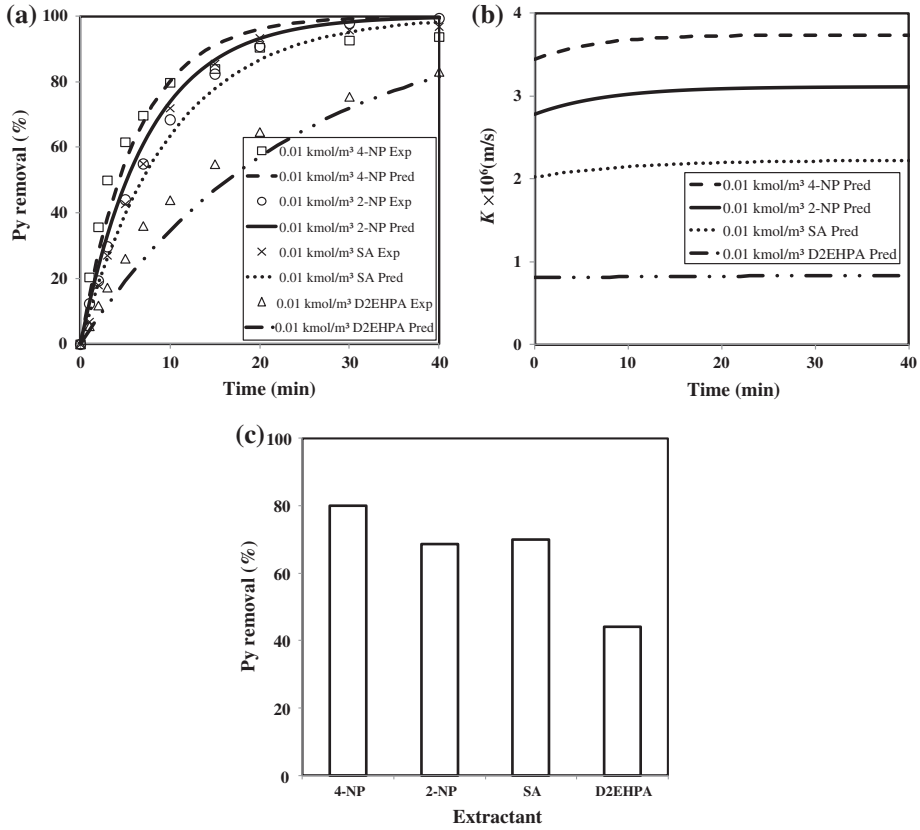

Fig. 7. Effect of different organic extractants (EXTs) on (a) pyridine removal (%), (b) overall mass transfer coefficient (K) and (c) pyridine removal vs. extractant at the end of 10 min (feed phase: 0.005 kmol/m^3 pyridine solution (500 ml); organic phase: 0.01 kmol/m^3 EXTs solution; strip phase: 0.1 kmol/m^3 HCl solution (500 ml); feed/strip phase flow rates: 200 ml/min, module 1).

As shown in Fig. 2, higher values of K_{ex} for pyridine at high pK_a of extractants corroborates to the fact that phenolic-based extractants have better ability to remove pyridine over conventional extractants. It has been reported that strong acids with protons that can participate in hydrogen bonding like, D2EHPA [31] and SA [32] form dimer in nonpolar solvents like kerosene, hexane, etc. As a result, although D2EHPA and SA are more acidic the acid groups are not available for complexation with the pyridine molecules. The comparative study of removal of pyridine for different extractants based on overall mass transfer coefficient (K) is shown in Fig. 7(b). The figure shows higher values of K for phenolic-based extractants compared to SA and D2EHPA. An increase in overall mass transfer coefficient (K) results into higher initial flux, which ultimately increases the extent of pyridine removal. The K values observed for the case with phenolic-based extractants (2-NP or 4-NP) are 3–4 times greater than SA and D2EHPA extractants. The results obtained in Table 3 and Fig. 7(b), show that high value of K_{ex} corresponds to higher mass transfer coefficient (K). Therefore, the fluxes observed with 4-NP and 2-NP extractants are higher compared to D2EHPA and SA extractants.

The relationship between extent of pyridine removal and different extractant is depicted in Fig. 7(c). It is observed from the figure that the phenolic-based extractants has the potential to remove pyridine faster compared to acidic extractants. Almost 98% removal of pyridine is achieved using 4-NP extractant. However, acidic extractants such as D2EHPA takes longer to achieve complete removal of pyridine.

4.8. Scale-up study

The effect of membrane scale on pyridine removal is studied using Module 1 and Module 3, respectively. The detail specifications about the modules are mentioned in Table 1. This study is carried out at 0.005 kmol/m^3 pyridine and 0.01 kmol/m^3 4-NP

concentrations. The feed/strip volume in large-scale module (Module 3) was four times than small-scale module (Module 1). The relationship between extent of pyridine removal and time for different module scales is shown in Fig. 8(a). It can be seen from the figure that, model predictions are in good agreement with the experimental observations. Fig. 8(a) shows nearly similar experimental trends of pyridine removal. The flux values obtained for 0.005 kmol/m^3 pyridine through Module 1 and Module 3 are 7.22×10^{-9} kmol/m^2 s and 7.92×10^{-9} kmol/m^2 s, respectively. This behavior can be explained from the plot between overall mass transfer coefficient (K) and time shown in Fig. 8(b). The overall mass transfer coefficient (K) does not show significant difference for both the scale of modules. As a result, similar trends of pyridine removal are observed in Fig. 8(a). Almost 75–80% pyridine removal is achieved using both the scale of modules at the end of 10 min.

4.9. Comparison with previous work reported in the literature

This work is more towards technology development. Therefore, it is essential to compare the results obtained in this work with alternative technologies, such as adsorption, pervaporation, etc. The comparison enables the practicing engineers to judge the practical relevance and utility of this work. A summary of the initial flux, extent of pyridine removal, etc. for different organic extractants is given in Table 6. These values are also compared with the values reported in the previous literature. The adsorption studies with different adsorbent [6,7] show lower values of flux compared to present study. The pervaporation experiments with PDMS membranes [14] show higher values of flux because these experiments were carried out with higher concentration of pyridine (0.3 kmol/m^3 pyridine concentration). This concentration is 10 times greater than the present work and is not relevant for separation of pyridine from dilute aqueous waste streams. At lower concentrations of pyridine, the flux values reported by Singha et al. [15] using pervaporation technique are similar in magnitude with the present work (Table 6). It is also seen from Table 6 that 4-NP and 2-NP extractants are most efficient from the point of view of faster removal of pyridine, since they give 95–98% removal at the end of 15 min. It can be seen that the flux observed in the present work is similar to those observed in case of pervaporation. This implies that the surface area of membranes to be used for application would be of similar size. The value of diffusivity in SLMs is higher than those in pervaporation. This means that concentration driving force is substantially higher in pervaporation processes. This happens because the solute partitioning in a pervaporation membrane can be substantially higher.

The advantage of the SLM technique while compared with the two extraction process with two contactors (extraction of the contaminated water with the selected organic phase (contactor 1) and then stripping of the organic phase with HCl (contactor 2)) is that a single unit does the job of extraction and separation. The quantity of organic extractant required is thus very small, 15 ml for 4-NP diluted in kerosene case. If we consider the two contactor system, the solvent requirement would be of the same order of magnitude as the feed volume (500 ml).

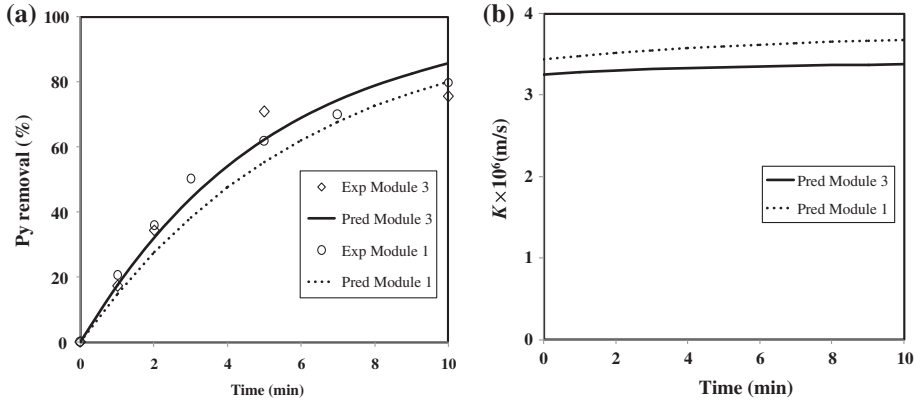

Fig. 8. Effect of scale on (a) pyridine removal (%) and (b) overall mass transfer coefficient (K) (feed phase: 0.005 kmol/m^3 pyridine solutions (500–2,000 ml); organic phase: 0.01 kmol/m^3 4-NP solution; strip phase: 0.1 kmol/m^3 HCl solution (500–2,000 ml); feed/strip phase flow rates: 200–500 ml/min).

Table 5
Effect of hollow fiber module parameters

Module parameter		Overall mass transfer coefficient (K) × 10^6 (m/s)	Pyridine removal (%) (within 15 min)
Porosity	0.2	2.03	51.56
	0.4	2.12	75.21
	0.6	2.17	86.62
Fiber/tube length (m)	0.15	2.12	75.21
	0.30	2.07	91.72
	0.45	2.01	96.62
Membrane thickness × 10^5 (m)	1	4.57	94.22
	3	2.12	75.21
	5	1.34	60.02

Note: This study is carried out at 0.01 kmol/m^3 pyridine concentration and 0.01 kmol/m^3 SA extractant.

The present mass transfer model is compared with the permeability-based model [33]. The process parameters such as overall mass transfer coefficient (K), membrane diffusivity (D_m), and permeability coefficient (P) calculated from the respective models for different organic extractants are given in Table 7. It can be seen from Table 7 that the values of K and D_m calculated from the present model are nearly similar to the values of P and D_m calculated from the permeability-based model. It shows the model versatility. In

Table 6
Comparative study of pyridine removal

Pyridine	Extractant	Initial flux (kmol/m^2 s)	Removal of pyridine (%) (within 15 min)	Refs.
0.005 M	0.01 kmol/m^3 D2EHPA	0.45×10^{-8}	55.01	Present
	0.01 kmol/m^3 SA	0.75×10^{-8}	77.96	work
	0.05 kmol/m^3 SA	0.84×10^{-8}	81.55	
	0.01 kmol/m^3 2-NP (DD)	0.69×10^{-8}	79.58	
	0.01 kmol/m^3 2-NP	0.83×10^{-8}	82.51	
	0.01 kmol/m^3 4-NP	1.09×10^{-8}	84.08	
	0.05 kmol/m^3 4-NP	1.51×10^{-8}	93.30	
0.01 M	0.01 kmol/m^3 2-NP	1.78×10^{-8}	83.61	Present
	0.01 kmol/m^3 4-NP	2.35×10^{-8}	93.30	work
0.02 M	0.01 kmol/m^3 2-NP (DD)	1.25×10^{-8}	78.43	Present
	0.05 kmol/m^3 2-NP	6.15×10^{-8}	97.89	work
0.03 M	0.01 kmol/m^3 2-NP (DD)	2.85×10^{-8}	72.90	Present
	0.05 kmol/m^3 2-NP	7.47×10^{-8}	97.51	work
~0.003 M	Adsorption (using 15 gm/dm^3 BFA	4.47×10^{-14}	96.82	[6]
~0.004 M	adsorbent, within 6 h)	6.40×10^{-14}	92.38	
~0.004 M	Adsorption using (a) 60 gm/dm^3 RHA adsorbent, within 5 h	5.00×10^{-14}	93.18	[7]
	(b) 60 gm/dm^3 GAC adsorbent, within 6 h	1.66×10^{-14}	97.31	
0.3 M	Pervaporation (PDMS membrane)	60.4×10^{-8}	–	[14]
0.06 M	Pervaporation (SBR membrane)	4.64×10^{-8}	–	[15]
0.12 M		5.618×10^{-8}		

Notes: In all the cases extractants have been diluted in kerosene except in some of the cases dodecane (DD) is used as diluent. Membrane diffusivity (D_m) = 3×10^{-10} m^2/sec, PDMS = polydimethylsiloxane, SBR = styrene butadiene rubber, BFA = bagasse fly ash, RHA = rice husk ash, GAC = granular activated carbon.

Table 7
Comparison of present model with permeability-based model

Extractants	Present model		Permeability-based model	
	Overall M.T. coefficient (K), (m/s) × 10^8	Membrane diffusivity (D_m), (m^2/s) × 10^{10}	Permeability (P), (m/s) × 10^8	Membrane diffusivity (D_m), (m^2/s) × 10^{10}
4-NP	367	3	373	2.5
2-NP	311	3	304	2.36
SA	214	3	212	2.53
D2EHPA	81.5	3	82	2.75

Note: This study is carried out at 0.005 kmol/m^3 pyridine with different organic extractants.

literature kinetic-based models are reported [34–37]. It is already explained in Section 4.1 that the transport process of pyridine is controlled by mass transfer resistances across the membrane. Therefore, the kinetic-based models are not suitable here for pyridine removal case.

5. Conclusions

The results obtained in this work have shown that pyridine can be removed using SLM technique. Equilibrium studies showed that phenolic-based solvents (4-NP or 2-NP) are better extractants for pyridine removal compared to SA and D2EHPA. The pK_a values, steric hindrance, dimerization, and overall mass transfer resistance are the key factors affecting the extent of pyridine removal. Phenolic extractants were able to remove almost 99% of the pyridine from feed. A mathematical model has been used to predict the transport of pyridine from feed to the strip side for three different modules. The model predictions are in good agreement with the experimental data. Also the results obtained from the scale-up study show good match between experimental and predicted data. This shows the used model is generalized and versatile in nature. The results could be explained on the basis of extraction equilibrium constant and membrane diffusivity. The results obtained from the kinetics study show that the kinetics of pyridine-complexation is much faster as compared with the residence times and the mass transfer rates in the hollow fiber module. This means that mass transfer is a controlling step in pyridine removal. The present study proves that HFSLM technique is better over the conventional technique as there is negligible loss and very less extractant consumption. The methodology proposed in the present work can be successfully applied to study the process of removal using SLMs.

Acknowledgment

The authors are grateful to the Department of Science and Technology (DST), Government of India, for providing financial assistance to research work through DST project (DST No.: SR/S3/CE/048/2012).

Nomenclature

C_{f0} — bulk concentration of the pyridine in the feed reservoir or the bulk inlet concentration of the pyridine in the feed-side (lumen-side) fluid at the fiber inlet (kmol/m^3)
$C_f(0)$ — bulk concentration of the pyridine in the feed reservoir at initial time (t = 0), (kmol/m^3)
$C_f(t)$ — bulk concentration of the pyridine in the feed reservoir at any time (t > 0), (kmol/m^3)
C_f — bulk concentration of the pyridine in the feed-side (lumen-side) fluid at location "Z = 0" (kmol/m^3)
C_{fz} — bulk concentration of the pyridine in the feed-side (lumen-side) fluid at location $Z = L$ (kmol/m^3)
C_{if} — concentration of the pyridine in the feed-side (lumen-side) fluid at feed-membrane interface (kmol/m^3)
C_{imf} — concentration of the pyridine complex in the supported liquid (membrane-fluid) at feed-membrane interface (kmol/m^3)
D — molecular diffusion coefficient of pyridine in the aqueous phases (m^2/s)
D_m — molecular diffusion coefficient of pyridine complex in the supported liquid (m^2/s)
K — overall mass transfer coefficient of pyridine molecule (m/s)
k — distribution coefficient of pyridine (–)
K_{ex} — extraction equilibrium constant of the pyridine complexation reaction (m^3/kmol)
k_f — feed-side film mass transfer coefficient (m/s)
L — effective length of the hollow fiber module (m)
r_{if} — inner radius of the hollow fiber tube (m)
R_T — mass transfer flux of the pyridine molecule (kmol /m^2 s)

R_{TCM} — mass transfer flux of the pyridine complex (kmol/m^2 s)
t — time (min)
T — temperature (K)
u_f — velocity of feed phase through lumen side of the module (m/s)
u_s — velocity of strip phase through shell side of the module (m/s)
v_A — solute molal volume at normal boiling point (m^3/kmol)
V_f — fluid volume in the feed phase reservoir (m^3)
V_s — fluid volume in the strip phase reservoir (m^3)
Q_f — feed-side volumetric flow rate (m^3/s)
d_0 — membrane thickness (m)
ε — porosity of the membranes (–)

References

[1] O.A. Zalat, M.A. Elsayed, A study on microwave removal of pyridine from wastewater, J. Environ. Chem. Eng. 1 (2013) 137–143.
[2] R.A. Baker, Threshold odors of organic chemicals, J. Am. Water Work 55 (1963) 913–916.
[3] A. Laitinen, M. Maukonen, Separation of pyridine or pyridine derivatives from aqueous solutions, EP1019341 A1, 2000.
[4] R. Lewis, Sax's Dangerous Properties of Industrial Materials, eleventh ed., John Wiley & Sons, New Jersey, NJ, 2004.
[5] A. Jori, D. Calamari, F. Cattabeni, A.D. Domenico, C.L. Galli, E. Galli, Ecotoxicological profile of pyridine, Ecotoxicol. Environ. Saf. 7 (1983) 251–275.
[6] D.H. Lataye, I.M. Mishra, I.D. Mall, Removal of pyridine from aqueous solution by adsorption on bagasse fly ash, Ind. Eng. Chem. Res. 45 (2006) 3934–3943.
[7] D.H. Lataye, I.M. Mishra, I.D. Mall, Pyridine sorption from aqueous solution by rice husk ash (RHA) and granular activated carbon (GAC): Parametric, kinetic, equilibrium and thermodynamic aspects, J. Hazard. Mater. 154 (2008) 858–870.
[8] Y. Bai, Q. Sun, R. Xing, D. Wen, X. Tang, Removal of pyridine and quinoline by bio-zeolite composed of mixed degrading bacteria and modified zeolite, J. Hazard. Mater. 181 (2010) 916–922.
[9] R. Anantharaj, T. Banerjee, Liquid–liquid equilibrium studies on the removal of thiophene and pyridine from pentane using imidazolium-based ionic liquids, J. Chem. Eng. Data 58 (2013) 829–837.
[10] K.V. Padoley, A.S. Rajvaidya, T.V. Subbarao, R.A. Pandey, Biodegradation of pyridine in a completely mixed activated sludge process, Bioresour. Technol. 97 (2006) 1225–1236.
[11] L. Qiao, J.L. Wang, Microbial degradation of pyridine by *Paracoccus* sp. isolated from contaminated soil, J. Hazard. Mater. 176 (2010) 220–225.
[12] W. Peng, H. Jiao, H. Shi, C. Xu, The application of emulsion liquid membrane process and heat-induced demulsification for removal of pyridine from aqueous solutions, Desalination 286 (2012) 372–378.
[13] E. Drioli, S. Zhang, A. Basile, Recovery of pyridine from aqueous solution by membrane pervaporation, J. Membr. Sci. 80 (1993) 309–318.
[14] P.C. Joyce, K.M. Devine, C.S. Slater, Separation of pyridine/water solutions using pervaporation, Sep. Sci. Technol. 30 (2006) 2145–2158.
[15] N.R. Singha, S. Ray, S.K. Ray, B.B. Konar, Removal of pyridine from water by pervaporation using filled SBR membranes, J. Appl. Polym. Sci. 121 (2011) 1330–1334.
[16] W. Kujawski, T.Q. Nguyen, J. Neel, Dehydration of water-pyridine mixtures by pervaporation, Sep. Sci. Technol. 26 (1991) 1109–1121.
[17] Y.M. Lee, B.K. Oh, Pervaporation of water-acetic acid mixture through poly(4-vinylpyridine-co-acrylonitrile) membrane, J. Membr. Sci. 85 (1993) 13–20.
[18] R. Kumar, I.M. Mishra, I.D. Mall, Treatment of pyridine bearing waste water using activated carbon, Res. Ind. 40 (1995) 33–37.
[19] H. Bludau, H.G. Karge, W. Niessen, Sorption, sorption kinetics and diffusion of pyridine in zeolites, Microporous Mesoporous Mater. 22 (1998) 297–308.
[20] E. Sabah, M.S. Çelik, Interaction of pyridine derivatives with sepiolite, J. Colloid Interface Sci. 251 (2002) 33–38.
[21] D. Mohan, K.P. Singh, S. Sinha, D. Gosh, Removal of pyridine derivatives from aqueous solution by activated carbons developed from agricultural waste materials, Carbon 43 (2005) 1680–1693.
[22] D. Mohan, K.P. Singh, S. Sinha, D. Gosh, Removal of pyridine from aqueous solution using low cost activated carbons derived from agricultural waste materials, Carbon 42 (2004) 2409–2421.
[23] J. Bokhove, B. Schuur, A.B. de Haan, Equilibrium study on the reactive liquid–liquid extraction of 4-cyanopyridine with 4-nonylphenol, Chem. Eng. Sci. 82 (2012) 215–222.
[24] J. Bokhove, T.J. Visser, B. Schuur, A.B. de Haan, Selective recovery of a pyridine derivative from an aqueous waste stream containing acetic acid and succinonitrile with solvent impregnated resins, React. Funct. Polym. 86 (2015) 67–79.
[25] M. Berthelot, C. Laurence, M. Safar, F. Besseau, Hydrogen-bond basicity pK_{HB} scale of six-membered aromatic N-heterocycles, J. Chem. Soc., Perkin Trans. 2 (1998) 283–290.
[26] P.K. Parhi, Supported liquid membrane principle and its practices: A short review, J. Chem. (2013) 1–11.
[27] A.K. Pabby, A.M. Sastre, State-of-the-art review on hollow fibre contactor technology and membrane-based extraction processes, J. Membr. Sci. 430 (2013) 263–303.
[28] P.V. Vernekar, Y.D. Jagdale, A.W. Patwardhan, A.V. Patwardhan, S.A. Ansari, P.K. Mohapatra, Non-dispersive solvent extraction of neodymium using N, N,N´,N´-tetraoctyl diglycolamide (TODGA), Sep. Sci. Technol. 49 (2014) 1541–1554.
[29] Y.D. Jagdale, P.V. Vernekar, A.W. Patwardhan, A.V. Patwardhan, S.A. Ansari, P.K. Mohapatra, V.K. Manchanda, Mathematical model for the extraction of metal ions using hollow fiber supported liquid membrane operated in a recycling mode, Sep. Sci. Technol. 48 (2013) 2454–2467.

[30] P.V. Vernekar, Y.D. Jagdale, A.W. Patwardhan, A.V. Patwardhan, S.A. Ansari, P.K. Mohapatra, V.K. Manchanda, Transport of cobalt(II) through a hollow fiber supported liquid membrane containing di-(2-ethylhexyl) phosphoric acid (D2EHPA) as the carrier, Chem. Eng. Res. Des. 91 (2013) 141–157.
[31] A. Mellah, D. Benachour, The solvent extraction of zinc and cadmium from phosphoric acid solution by di-2-ethyl hexyl phosphoric acid in kerosene diluent, Chem. Eng. Process. 45 (2006) 684–690.
[32] N. Garti, K. Sato, J. Schlichter, E. Wellner, The dimer association of stearic acid in solution, Cryst. Res. Technol. 21 (1986) 653–656.
[33] T. Pirom, N. Sunsandee, T. Wongsawa, P. Ramakul, U. Pancharoen, K. Nootong, The effect of temperature on mass transfer and thermodynamic parameters in the removal of amoxicillin via hollow fiber supported liquid membrane, Chem. Eng. J. 265 (2015) 75–83.
[34] Y. Jun, Y. Huh, W. Hong, Y. Hong, Kinetics of the extraction of succinic acid with tri-n-octylamine in 1-octanol solution, Biotechnol. Prog. 21 (2005) 1673–1679.
[35] M. Marti, T. Gurkan, L. Doraiswamy, Equilibrium and kinetic studies on reactive extraction of pyruvic acid with trioctylamine in 1-octanol, Ind. Eng. Chem. Res. 50 (2011) 13518–13525.
[36] S. Suren, U. Pancharoen, S. Kheawhom, Simultaneous extraction and stripping of lead ions via a hollow fiber supported liquid membrane: Experiment and modeling, J. Ind. Eng. Chem. 20 (2014) 2584–2593.
[37] K. Tang, J. Luo, P. Zhang, J. Yi, J. Hua, C. Yang, Kinetic study on reactive extraction of phenylalanine enantiomers with BINAP–copper complexes, Chin. J. Chem. Eng. 23 (2015) 57–63.